

Structural Characterization of Methylenedianiline Regioisomers by Ion Mobility and Mass Spectrometry I. Dimers

Jay G. Forsythe[†], Sarah M. Stow[†], Hartmut Nefzger[#], Nicholas W. Kwiecien[§], Jody C. May, John A. McLean*, and David M. Hercules*

Department of Chemistry, Vanderbilt University, Nashville, TN 37235

[†]Co-first authors

[#]Bayer MaterialScience AG, 51368 Leverkusen, Germany

[§]Present address: Department of Chemistry, University of Wisconsin, Madison, WI 53706

*Corresponding Authors: Department of Chemistry, Vanderbilt University, Nashville, TN 37235

Ph: 615-343-5230, E-mail: david.m.hercules@vanderbilt.edu.

Ph: 615-322-1195, E-mail: john.a.mclean@vanderbilt.edu

Abstract: Purified methylenedianiline (MDA) regioisomers were structurally characterized and differentiated using tandem mass spectrometry (MS/MS), ion mobility - mass spectrometry (IM-MS) and IM-MS/MS in conjunction with computational methods. It was determined that protonation sites on the isomers can vary depending on the position of amino groups, and the resulting protonation sites play a role in the gas-phase stability of the isomer. We also observed differences in the relative distributions of protonated conformations depending on experimental conditions and instrumentation, which is consistent with previous studies on aniline in the gas phase. This work demonstrates the utility of a multifaceted approach for the study of isobaric species, and elucidates why previous MDA studies may have been unable to detect and/or differentiate certain isomers. Such analysis may prove useful in the characterization of larger MDA multimeric species, industrial MDA mixtures, and methylene diphenyl diisocyanate (MDI) mixtures used in polyurethane synthesis.

Table of Contents

NMR Spectroscopy of Purified MDA Isomers	Pages 3-9
Supplemental Material as Noted in the Manuscript	Pages 10-11
Additional Computational Data	Pages 12-29

NMR Spectroscopy of Purified MDA Isomers

NMR experiments were acquired using a 14.0 T Bruker magnet equipped with a Bruker AV-III console operating at 600.13 MHz. All spectra were acquired in 5mm NMR tubes using a Bruker 5 mm TCI cryogenically cooled NMR probe. Chemical shifts were referenced internally to DMSO (2.49 ppm) which also served as the ^2H lock solvents. For 1D ^1H NMR, typical experimental conditions included 32K data points, 13 ppm sweep width, a recycle delay of 1.5 seconds and 64 scans. For 1D ^{13}C NMR, typical experimental conditions included 32K data points, 250 ppm sweep width, 20° excitation pulse, a recycle delay of 2 seconds and 512 scans. Multiplicity-edited HSQC experiments were acquired using a 1024 x 256 data matrix, a J(C-H) value of 145 Hz which resulted in a multiplicity selection delay of 34 ms, a recycle delay of 1.5 seconds and 64 scans per increment along with GARP decoupling on ^{13}C during the acquisition time (150 ms). The data was processed using a p/2 shifted squared sine window function and displayed with CH/ CH_3 signals phased positive and CH_2 signals phased negative.

¹H NMR of 4,4'-MDA in DMSO

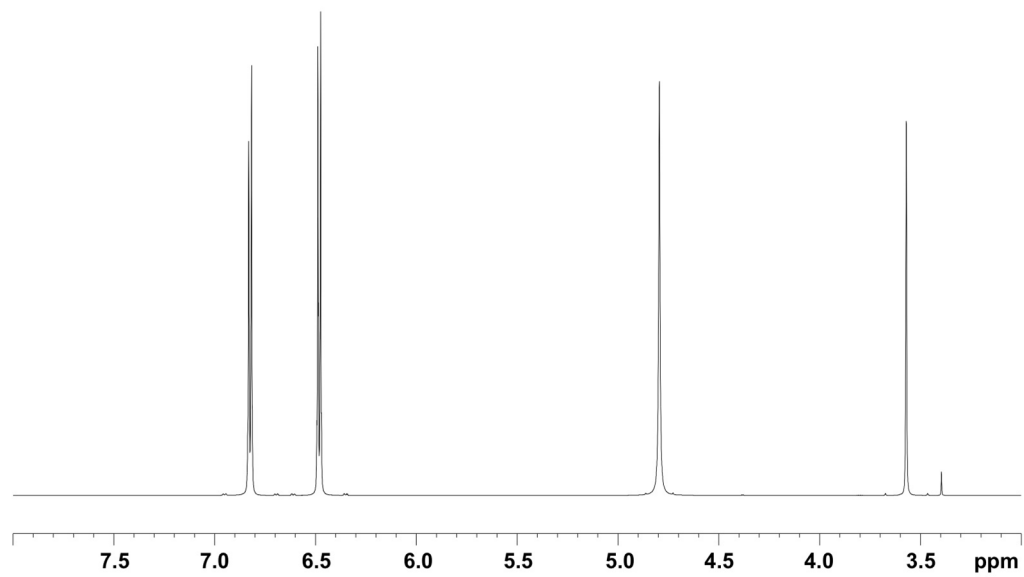


Figure S-1. ¹H NMR of 4,4'-MDA.

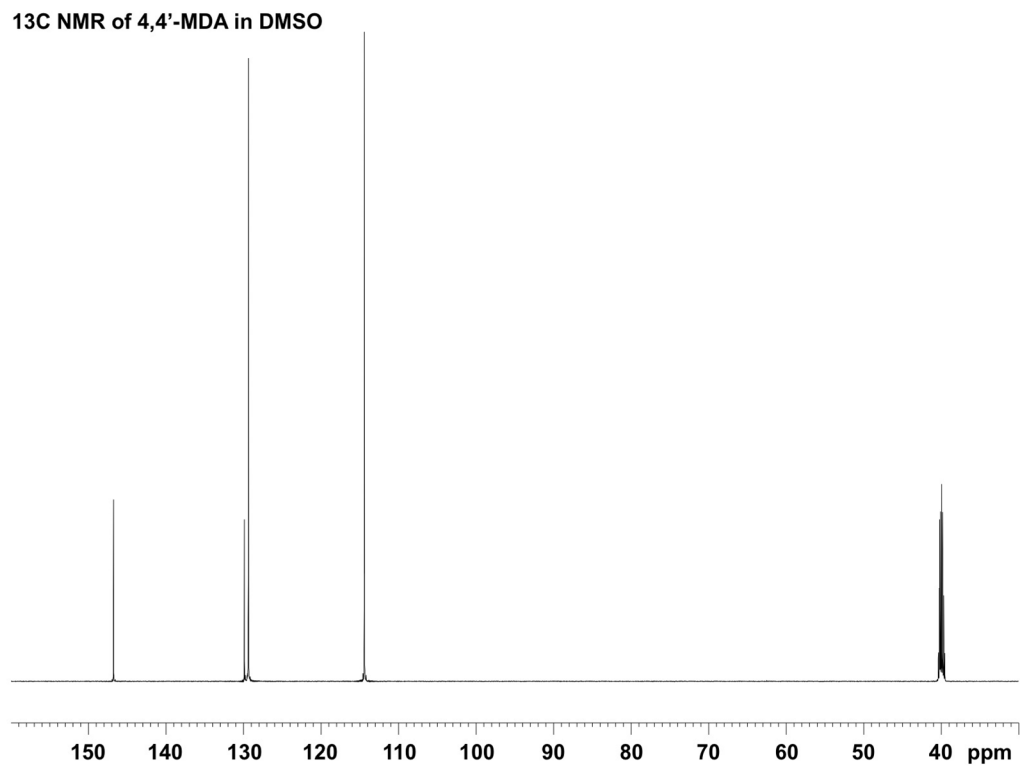


Figure S-2. ¹³C NMR of 4,4'-MDA.

¹H NMR of 2,2'-MDA in DMSO

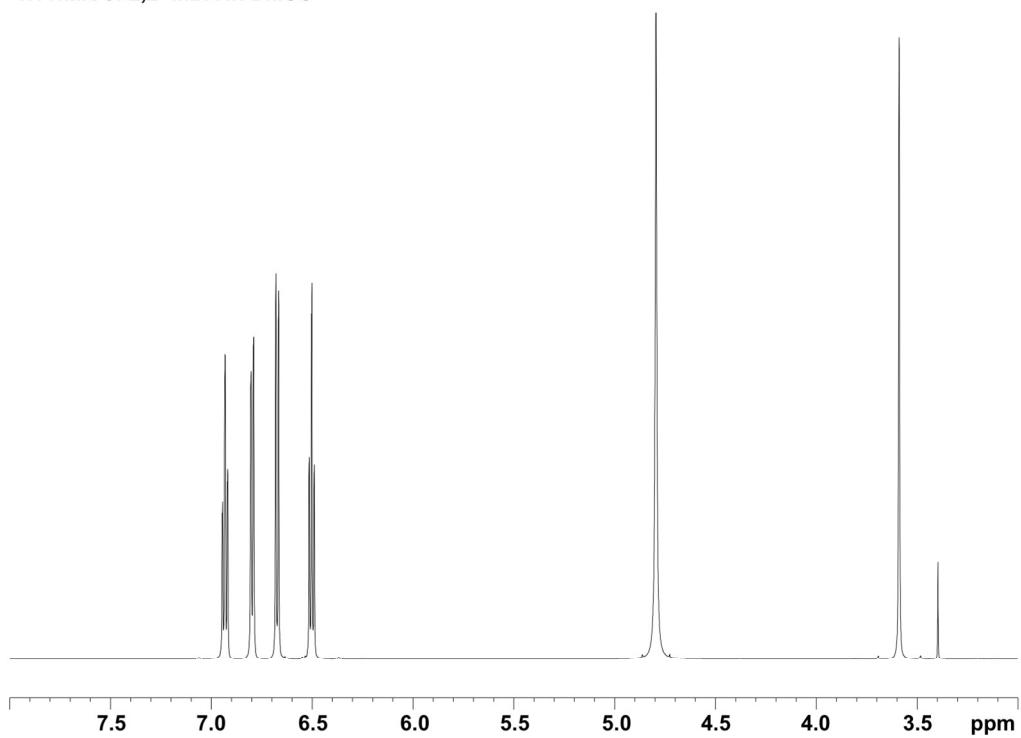


Figure S-3. ¹H NMR of 2,2'-MDA.

¹³C NMR of 2,2'-MDA in DMSO

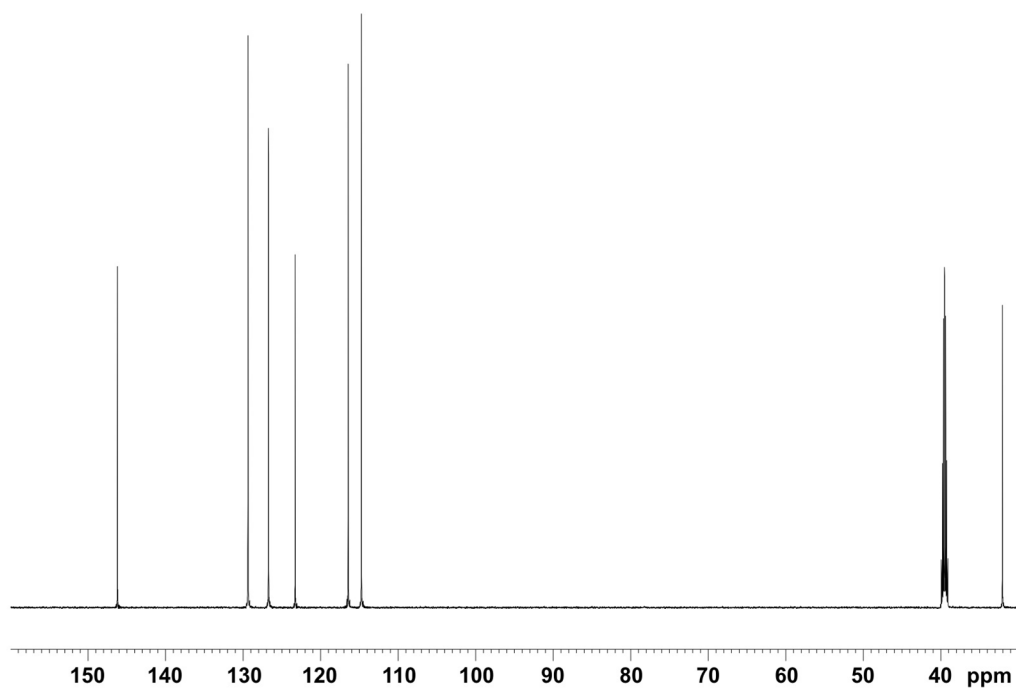


Figure S-4. ¹³C NMR of 2,2'-MDA.

^1H NMR of 2,4'-MDA in DMSO

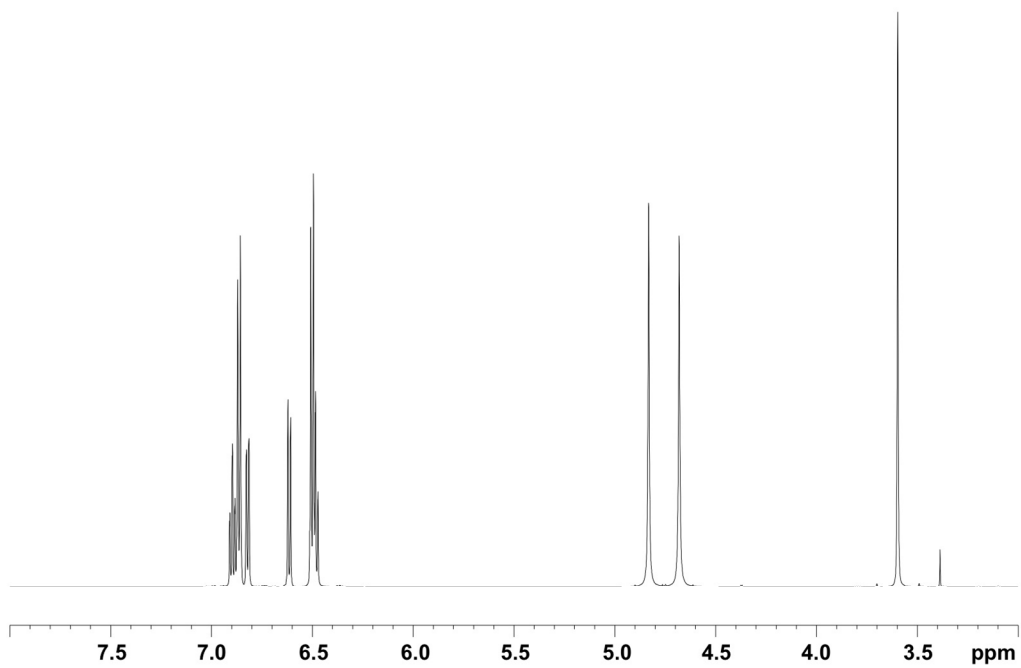


Figure S-5. ^1H NMR of 2,4'-MDA.

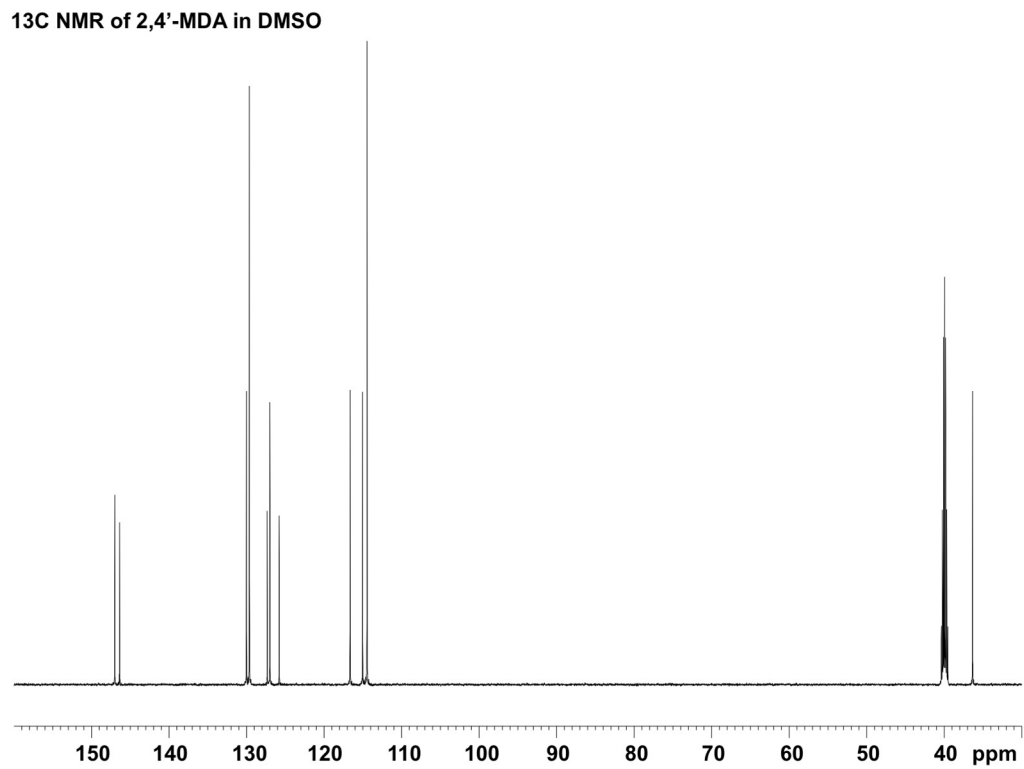


Figure S-6. ¹³C NMR of 2,4'-MDA.

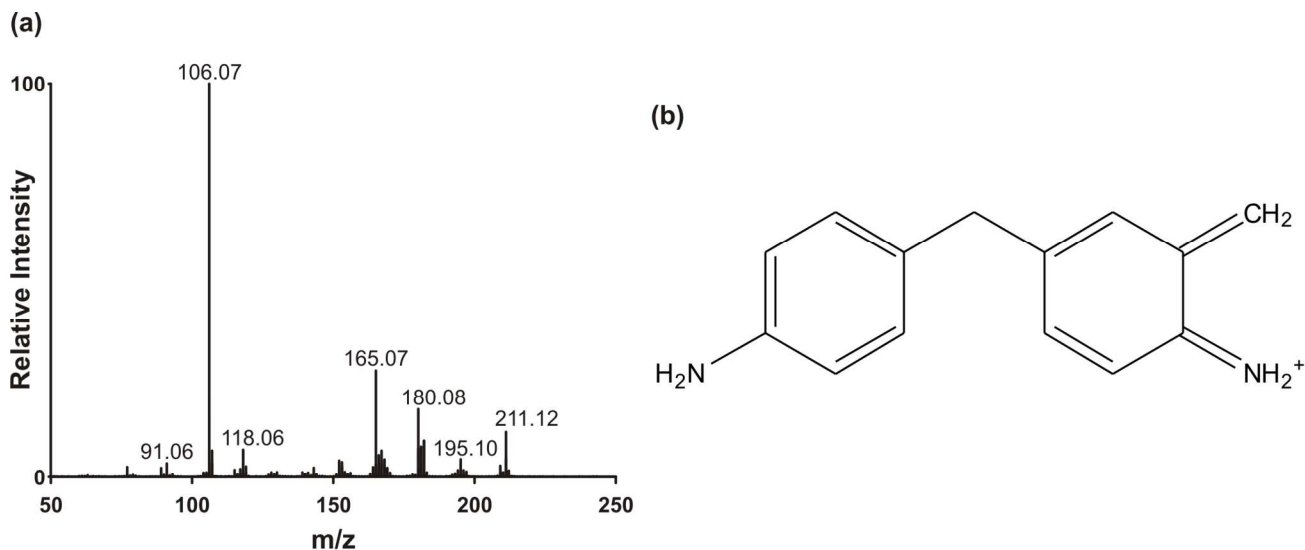


Figure S-7. (a) Tandem mass spectrum for 211 Da observed in the 4,4'-MDA sample. ESI ionization was used. A center-of-mass collision energy of 4.9 eV was applied (40 eV lab-frame). (b) Proposed structure for the 211 Da species. Most fragment signals for 211 Da match the 199 Da fragments shown in **Table 1** in the main text. The likely source of this ion is a very low abundance multimer which fragments into the 211 Da structure.

[M+H]⁺ Species	T-wave IM	DTIM
4,4'-MDA	97 ± 2%	99.89 ± 0.01%
2,2'-MDA	3.9 ± 0.1%	47.1 ± 0.2%
2,4'-MDA	0.9 ± 0.4%	37.6 ± 0.6%

Table S-1. Comparison of relative gas-phase stabilities between traveling-wave IM and DTIM instrument platforms. Values reflect the percent abundance of the 199 Da parent ion relative to the 106 Da fragment. $n = 3$ for each value. For both instrument platforms, 4,4'-MDA is significantly more stable than 2,2'-MDA and 2,4'-MDA. However, in both cases 2,2'-MDA is slightly more stable than 2,4'-MDA.

Additional Computational Data

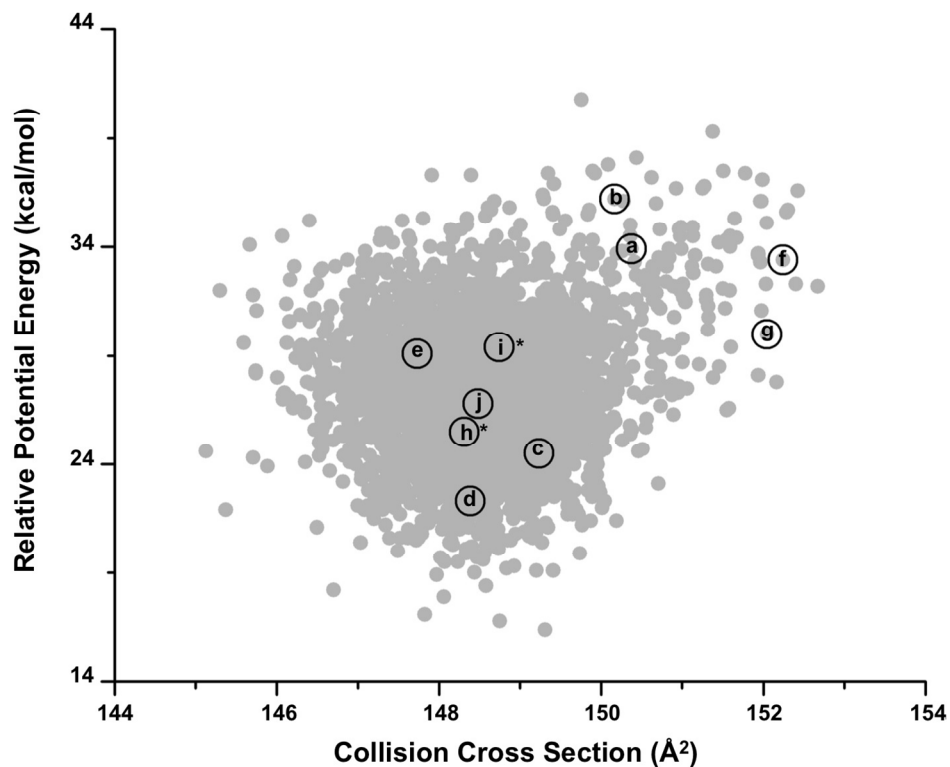


Figure S-8. Conformational space plot for the ortho amine protonated 2,2'-MDA. The 3,000 generated conformations are represented in grey, the clustering representative conformation are labeled with letters that correspond to the structures in Figures S-9 and S-10. The asterisk indicates the structures that are shown in the manuscript.

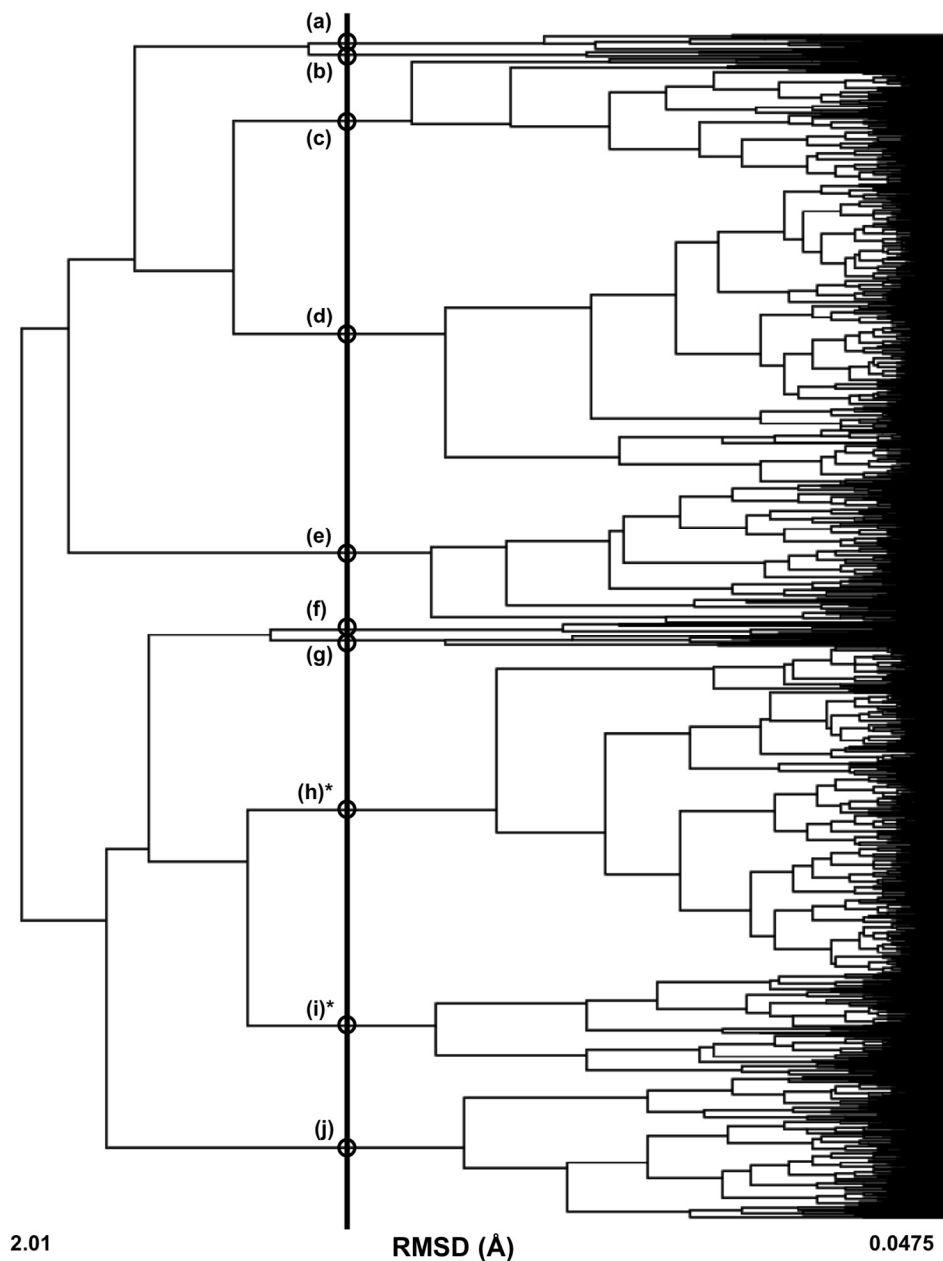


Figure S-9. Clustering analysis of 3,000 conformations of the ortho amine protonated 2,2'-MDA. Clustering is based on root mean square distance of atoms of superimposed structures. The vertical black bar indicates the RMSD cutoff (1.20 Å) used to select the conformations (circled) for further analysis. The asterisk represents the structures shown in the paper.

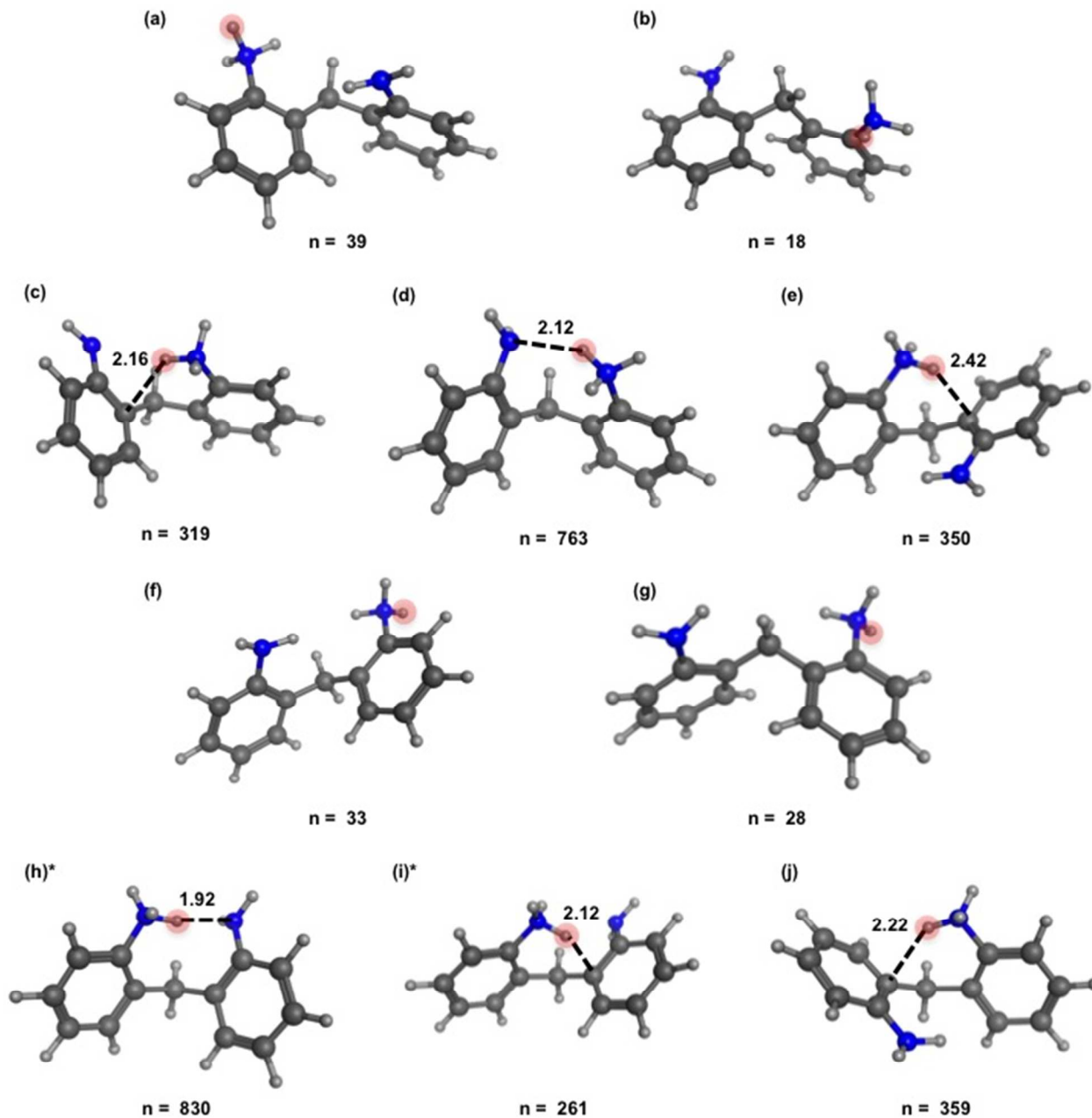


Figure S-10. Representative conformations of the ortho amine protonated 2,2'-MDA generated from an elevated temperature molecular dynamic protocol. Carbon atoms are shown in dark grey, hydrogen in light grey, and nitrogen in blue. The asterisk represents the structures shown in the paper. The number of conformations each of these represents from clustering is shown below the conformation.

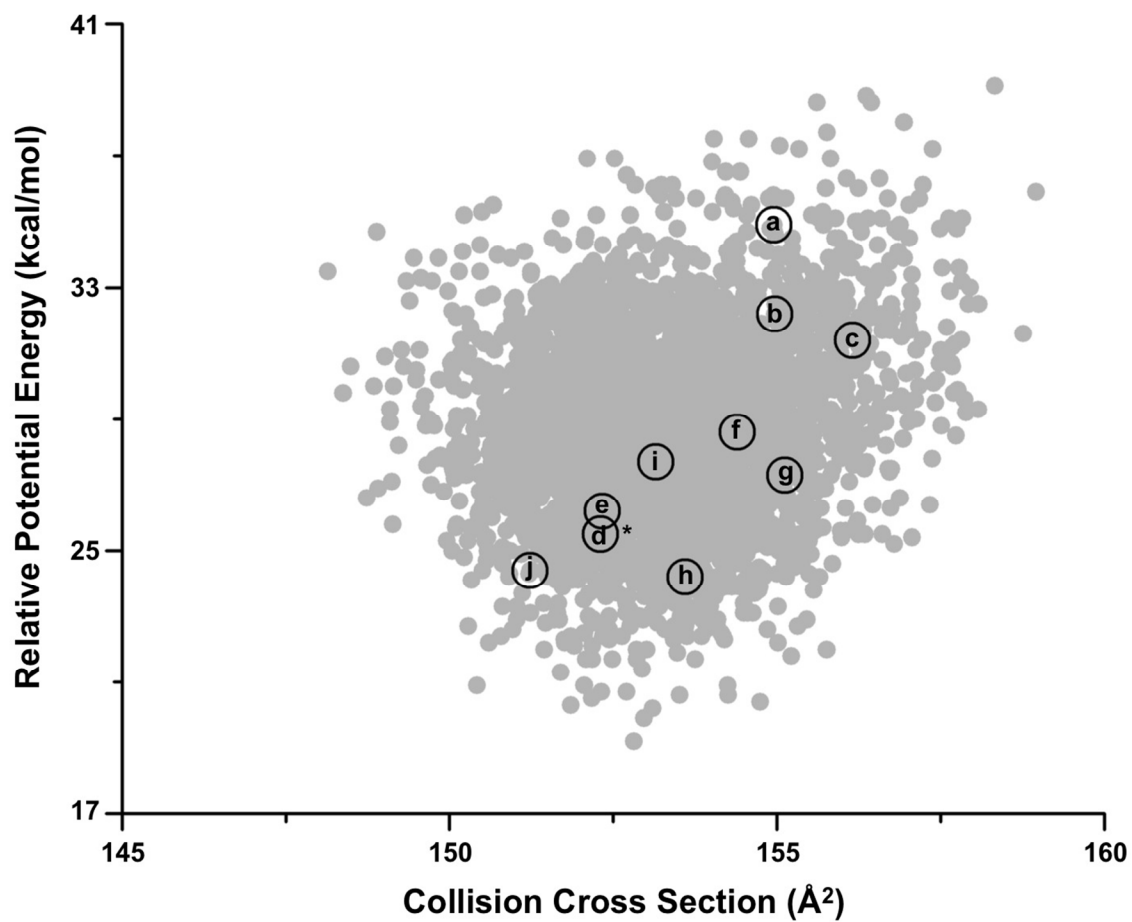


Figure S-11. Conformational space plot for ortho amine protonated 2,4'-MDA. The 3,000 generated conformations are represented in grey, the clustering representative conformation are labeled with letters that correspond to the structures in Figures S-12 and S-13. The asterisk indicates the structures that are shown in the manuscript.

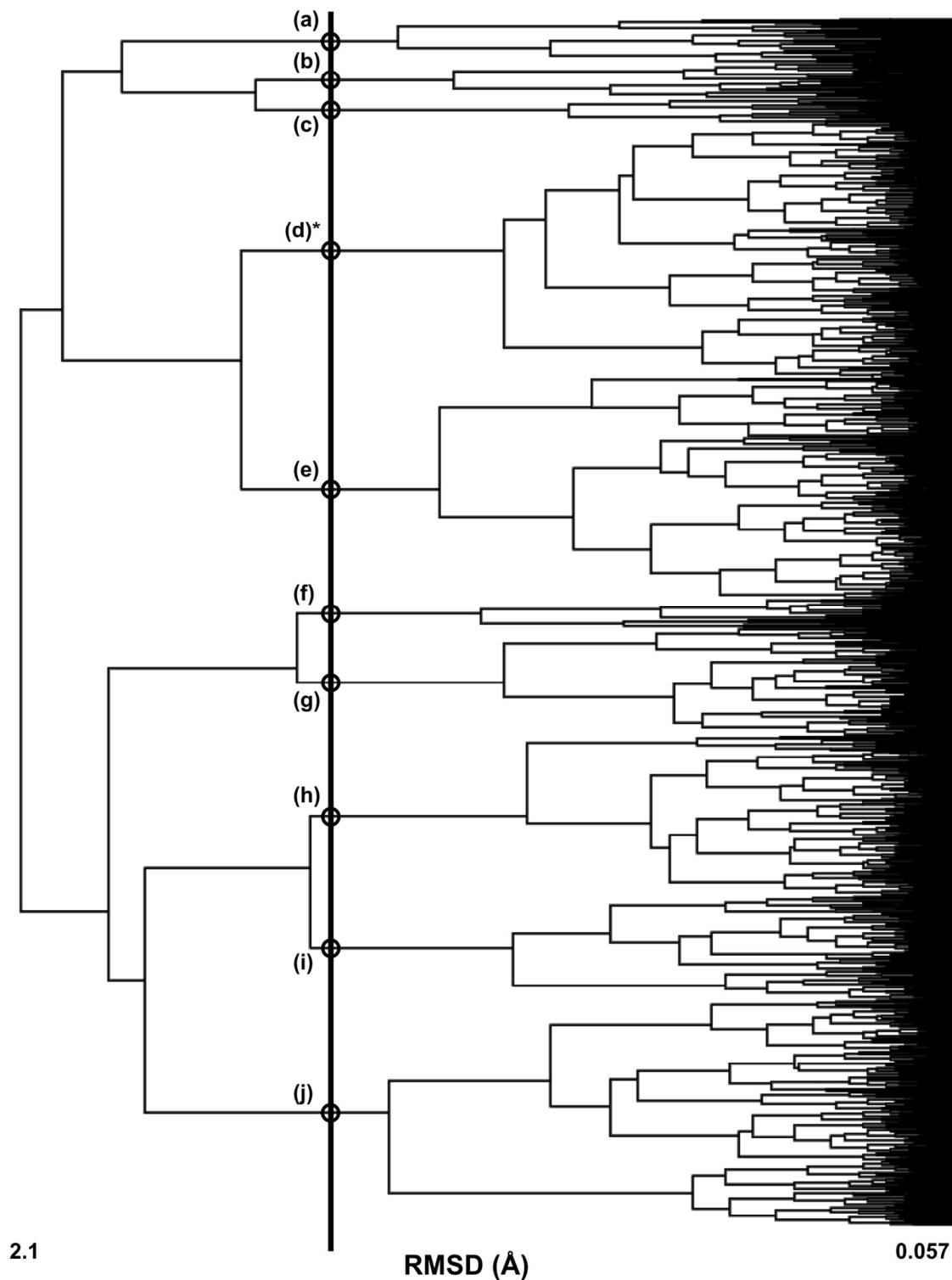


Figure S-12. Clustering analysis of 3,000 conformations of the ortho amine protonated 2,4'-MDA. Clustering is based on root mean square distance of atoms of superimposed structures. The vertical black bar indicates the RMSD cutoff (1.35 Å) used to select the conformations (circled) for further analysis. The asterisk represents the structures shown in the paper.

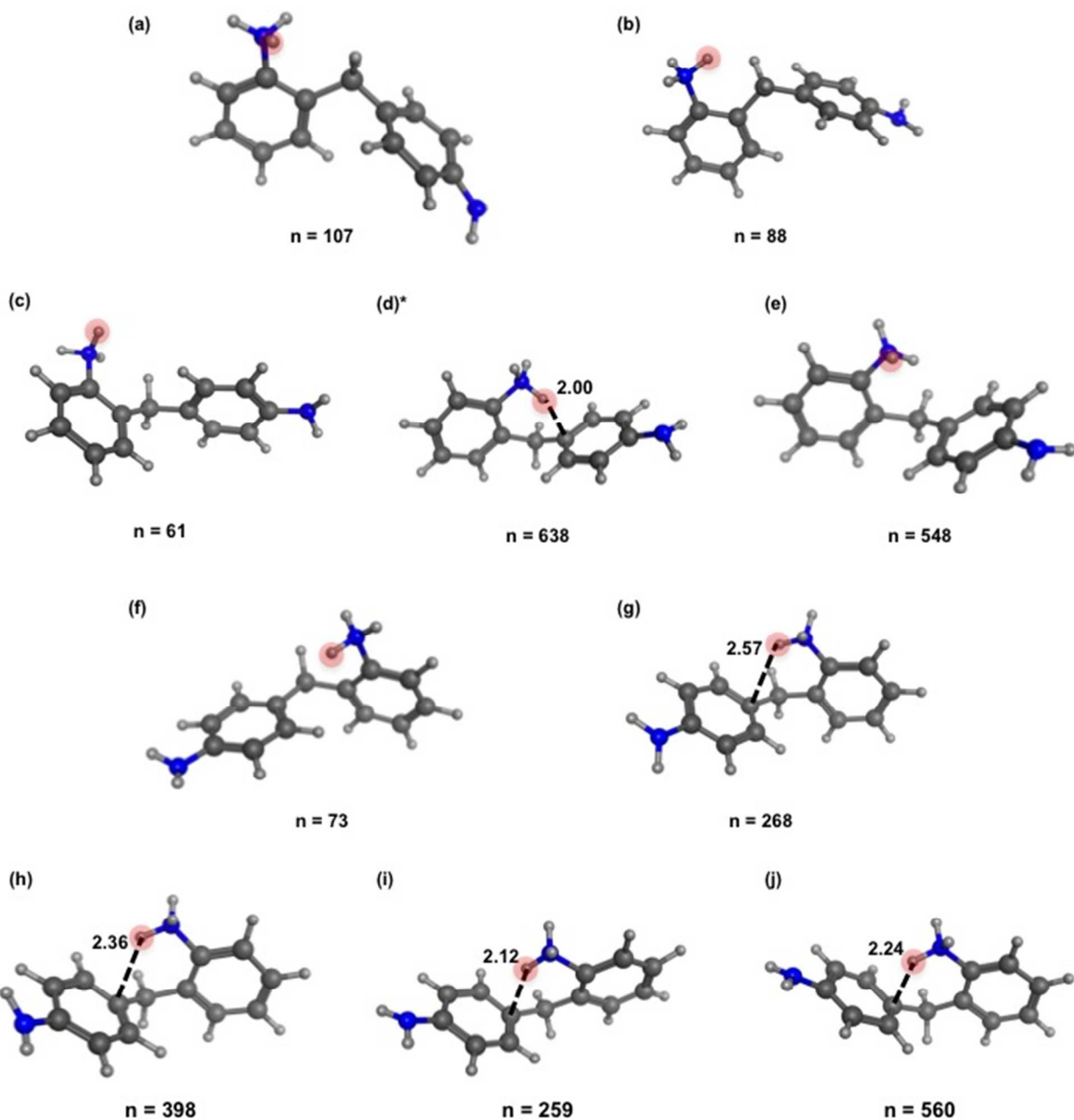


Figure S-13. Representative conformations of the ortho amine protonated 2,4'-MDA generated from an elevated temperate molecular dynamic protocol. Carbon atoms are shown in dark grey, hydrogen in light grey, and nitrogen in blue. The asterisk represents the structures shown in the paper. The number of conformations each of these represents from clustering is shown below the conformation.

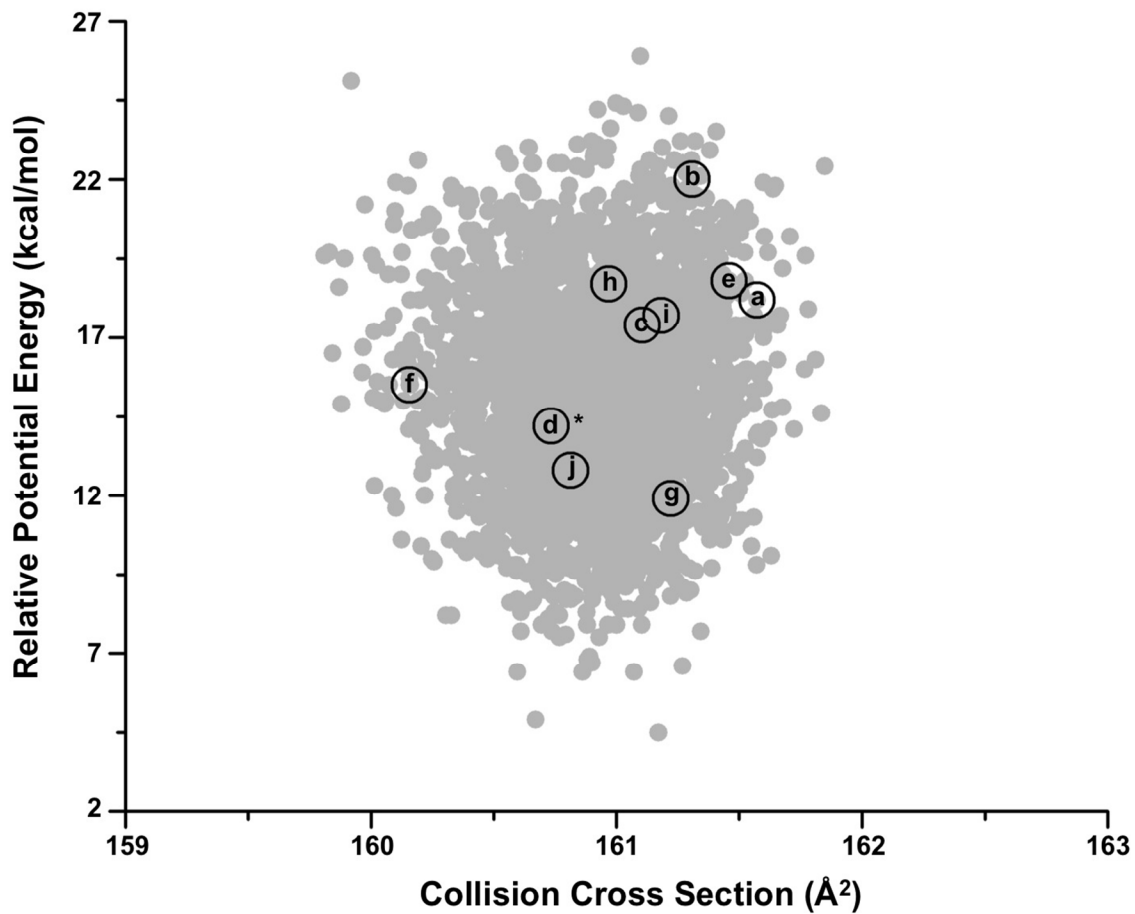


Figure S-14. Conformational space plot for the para amine protonated 4,4'-MDA. The 3,000 generated conformations are represented in grey, the clustering representative conformation are labeled with letters that correspond to the structures in Figures S-15 and S-16. The asterisk indicates the structures that are shown in the manuscript.

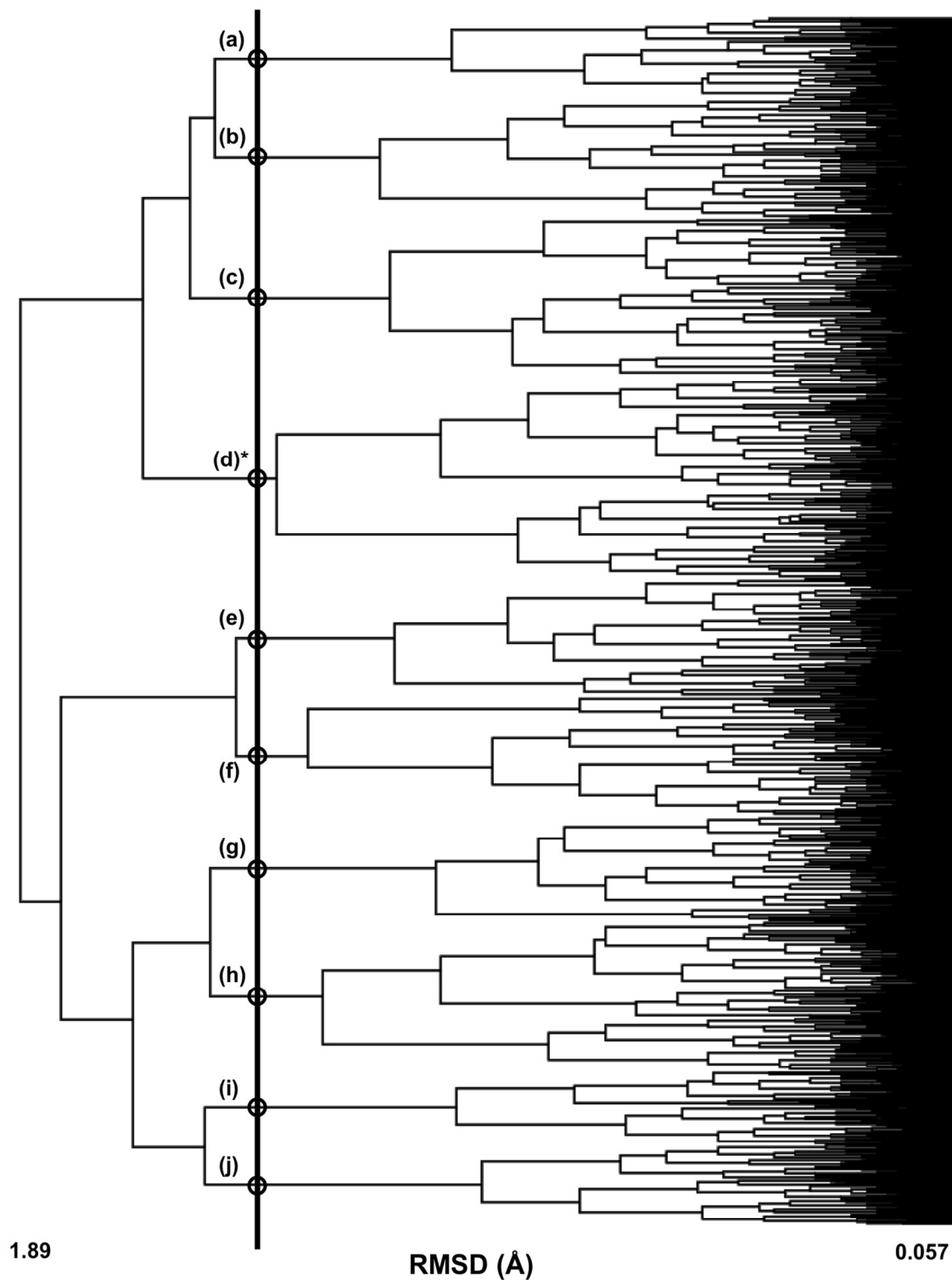


Figure S-15. Clustering analysis of 3,000 conformations of the para amine protonated 4,4'-MDA. Clustering is based on root mean square distance of atoms of superimposed structures. The vertical black bar indicates the RMSD cutoff (1.40 Å) used to select the conformations (circled) for further analysis. The asterisk represents the structures shown in the paper.

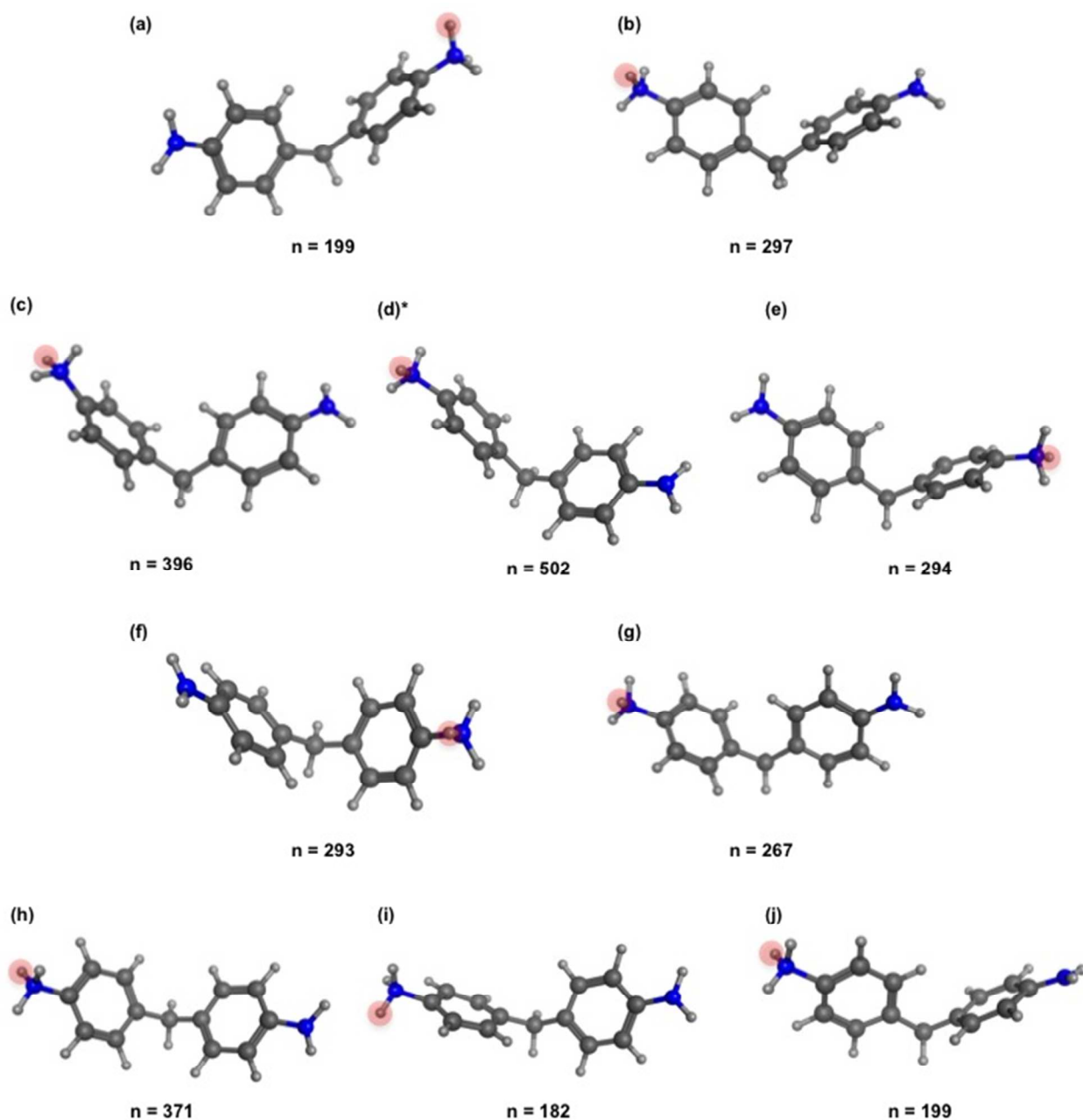


Figure S-16. Representative conformations of the para amine protonated 4,4'-MDA generated from an elevated temperate molecular dynamic protocol. Carbon atoms are shown in dark grey, hydrogen in light grey, and nitrogen in blue. The asterisk represents the structures shown in the paper. The number of conformations each of these represents from clustering is shown below the conformation.

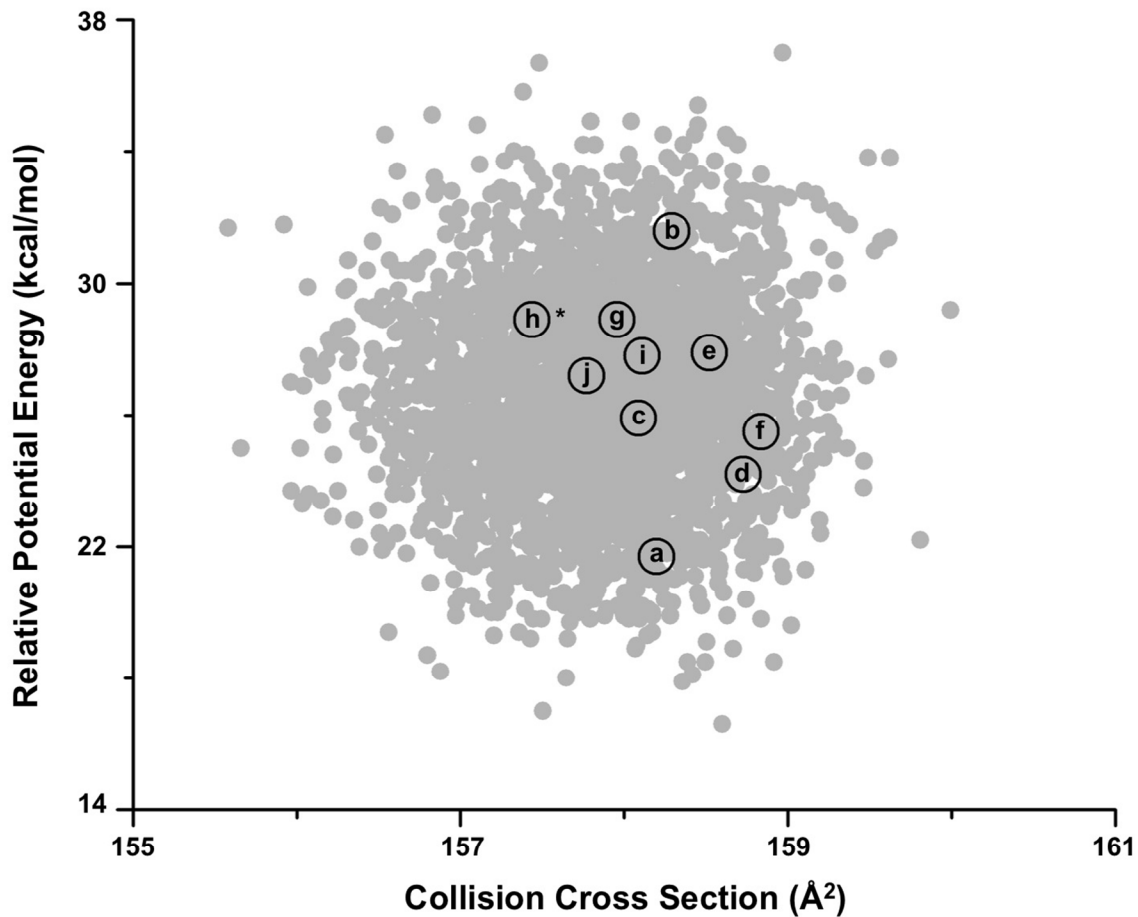


Figure S-17. Conformational space plot for the para amine protonated 2,4'-MDA. The 3,000 generated conformations are represented in grey, the clustering representative conformation are labeled with letters that correspond to the structures in Figures S-18 and S-19. The asterisk indicates the structures that are shown in the manuscript.

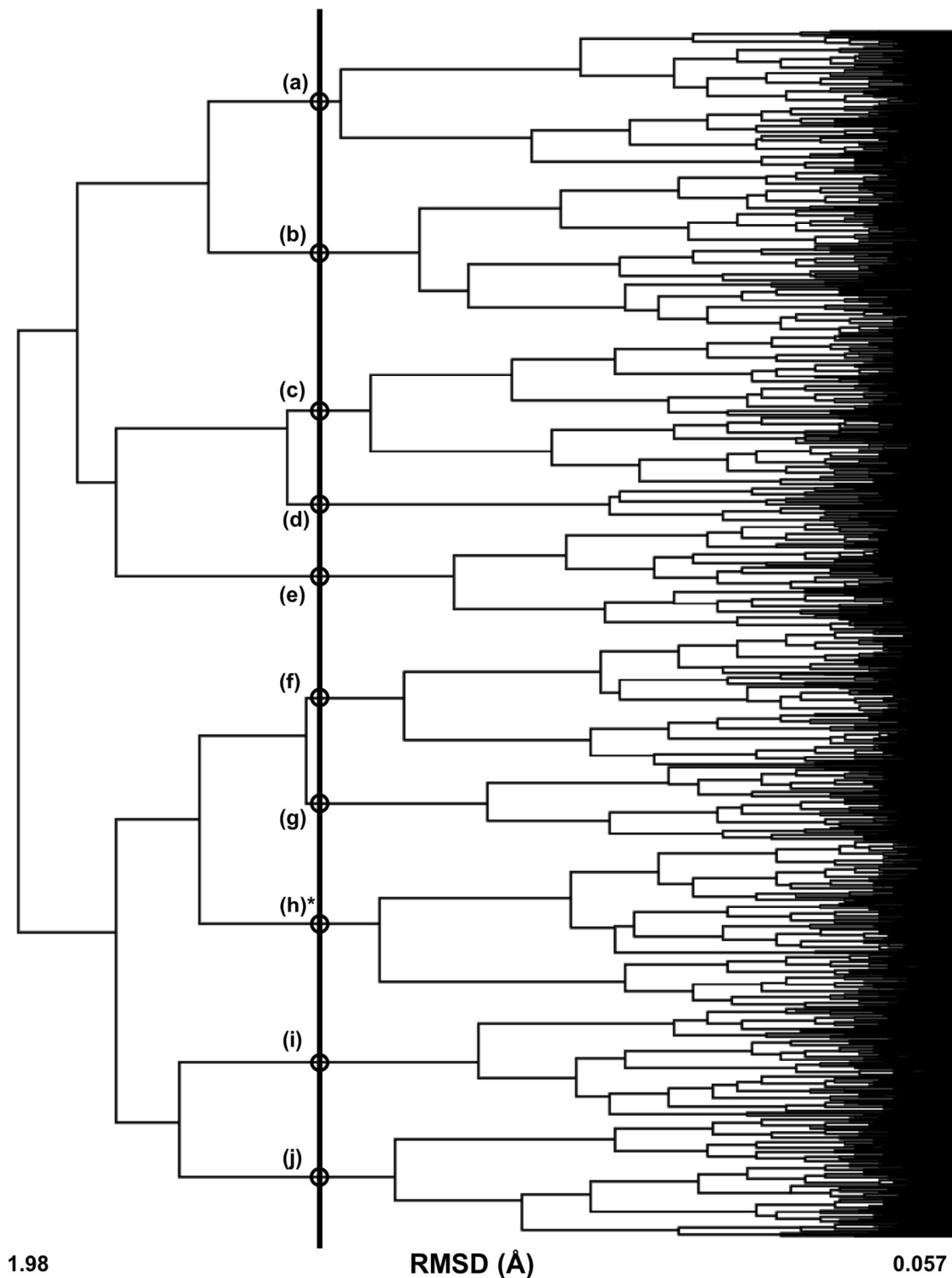


Figure S-18. Clustering analysis of 3,000 conformations of the para amine protonated 2,4'-MDA. Clustering is based on root mean square distance of atoms of superimposed structures. The vertical black bar indicates the RMSD cutoff (1.35 Å) used to select the conformations (circled) for further analysis. The asterisk represents the structures shown in the paper.

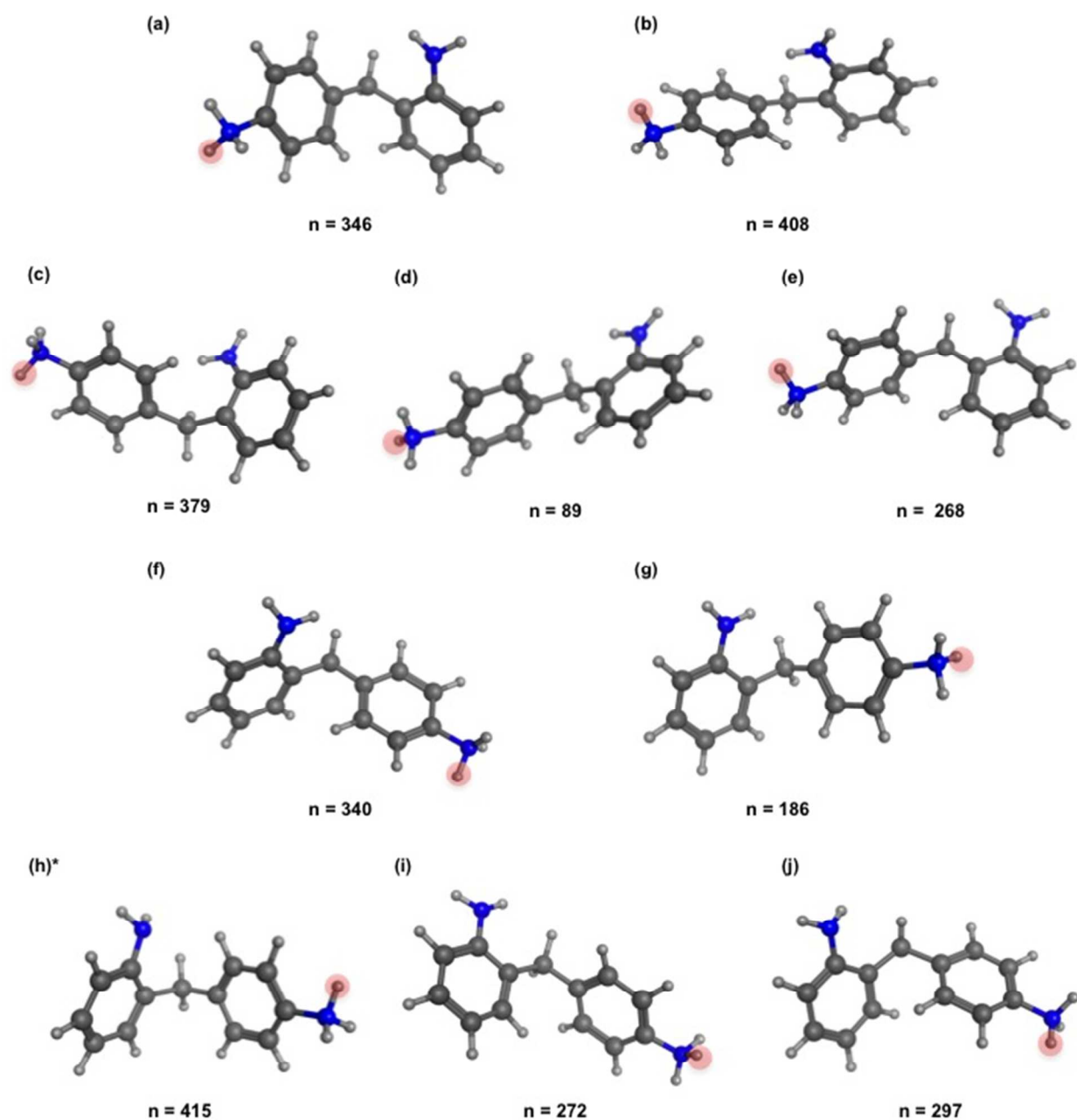


Figure S-19. Representative conformations of the para amine protonated 2,4'-MDA generated from an elevated temperate molecular dynamic protocol. Carbon atoms are shown in dark grey, hydrogen in light grey, and nitrogen in blue. The asterisk represents the structures shown in the paper. The number of conformations each of these represents from clustering is shown below the conformation.

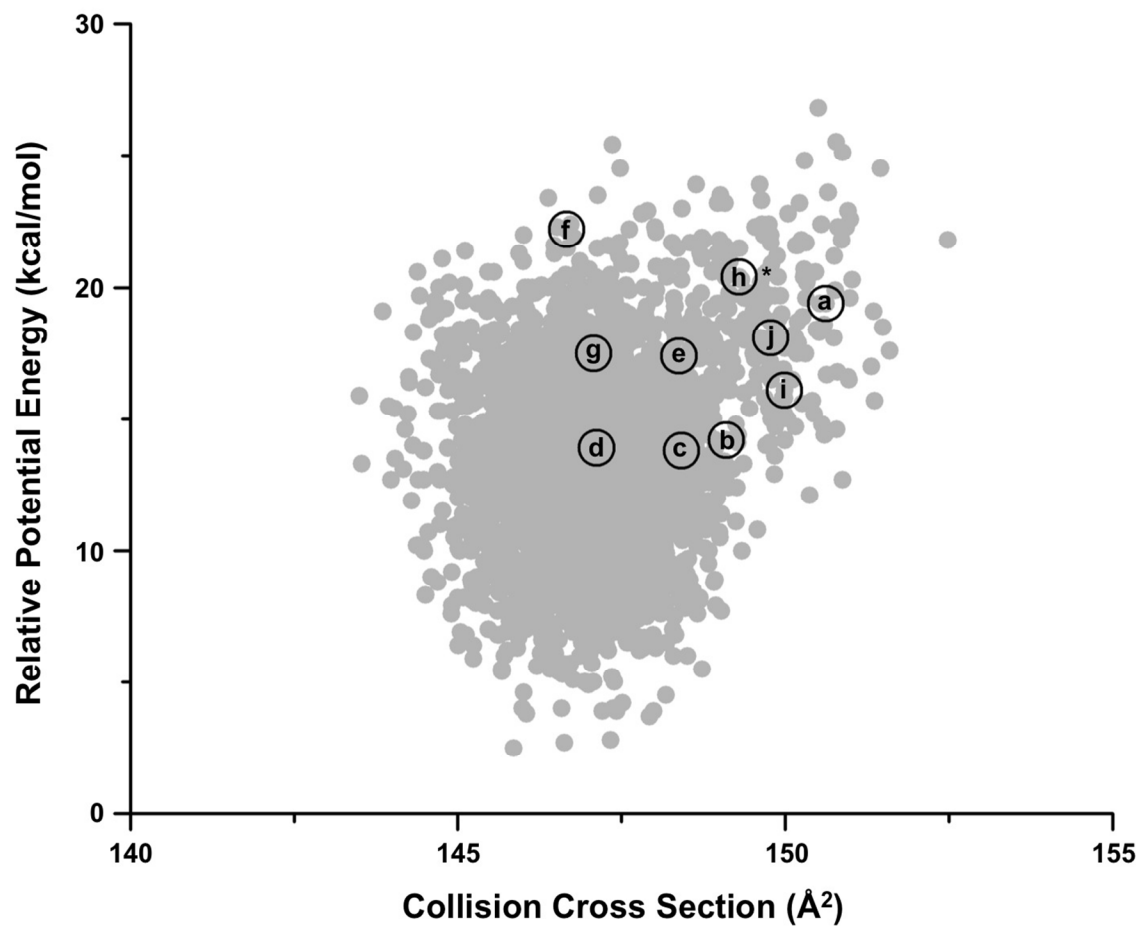


Figure S-20. Conformational space plot for the ring protonated 2,2'-MDA. The 3,000 generated conformations are represented in grey, the clustering representative conformation are labeled with letters that correspond to the structures in Figures S-21 and S-22. The asterisk indicates the structures that are shown in the manuscript.

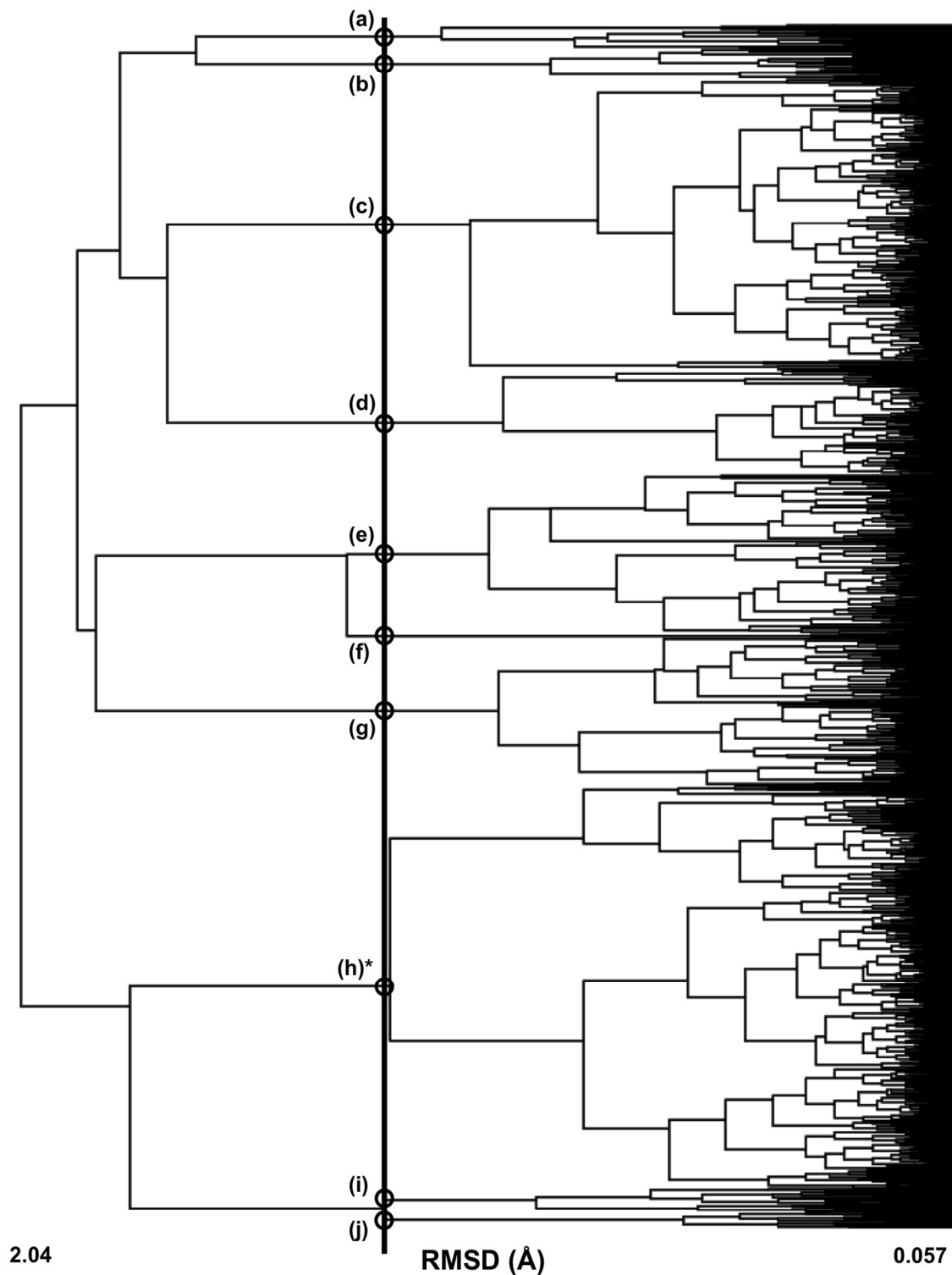


Figure S-21. Clustering analysis of 3,000 conformations of the ring protonated 2,2'-MDA. Clustering is based on root mean square distance of atoms of superimposed structures. The vertical black bar indicates the RMSD cutoff (1.26 Å) used to select the conformations (circled) for further analysis. The asterisk represents the structures shown in the paper.

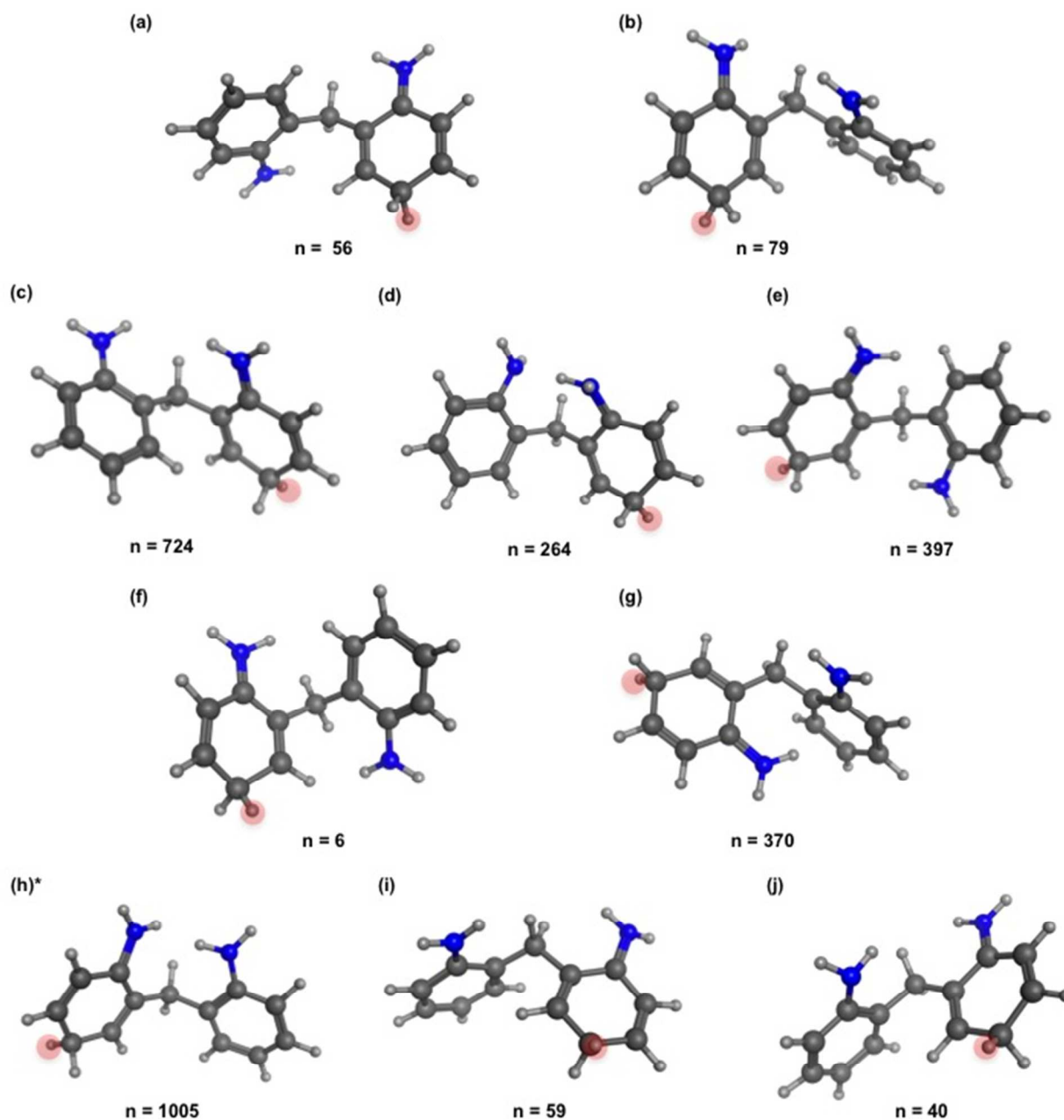


Figure S-22. Representative conformations of the ring protonated 2,2'-MDA generated from an elevated temperate molecular dynamic protocol. Carbon atoms are shown in dark grey, hydrogen in light grey, and nitrogen in blue. The asterisk represents the structures shown in the paper. The number of conformations each of these represents from clustering is shown below the conformation.

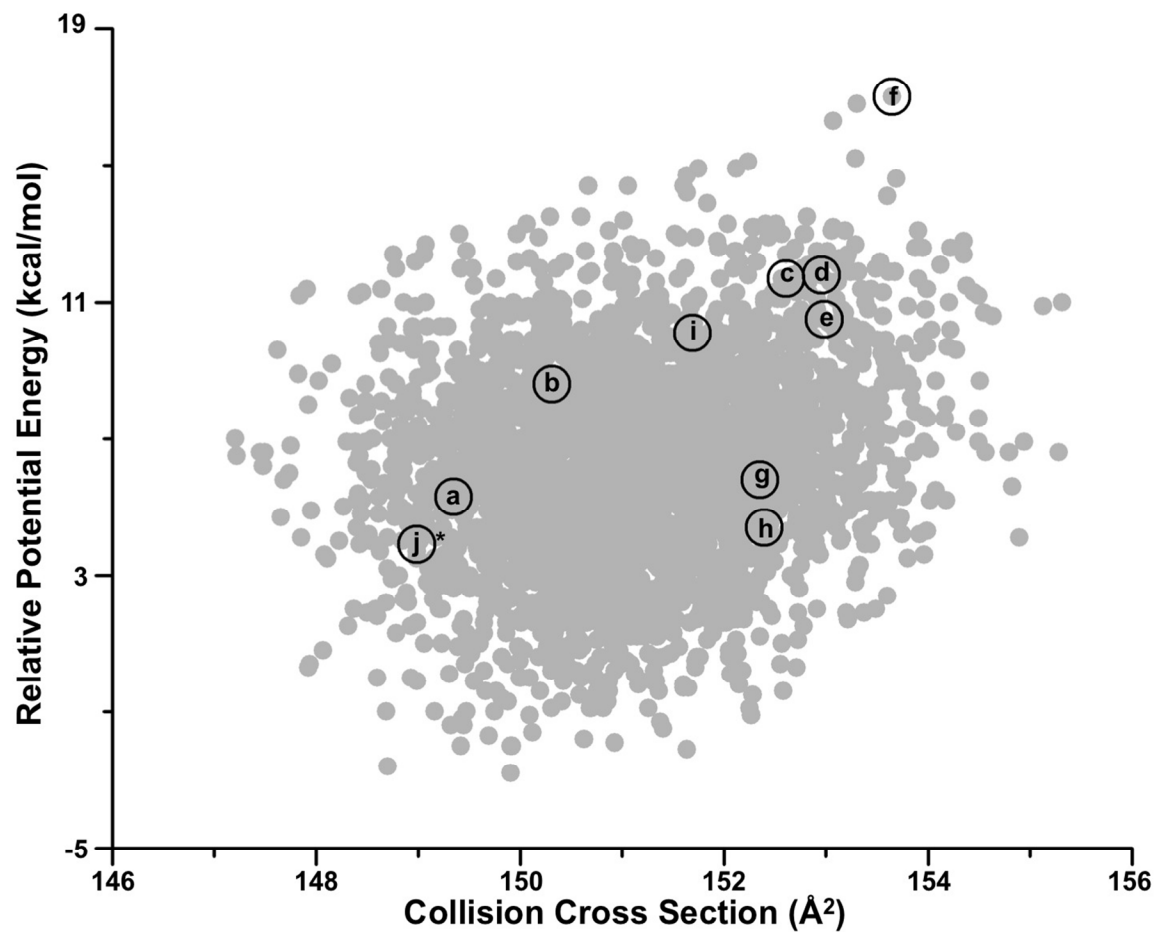


Figure S-23. Conformational space plot for the ring protonated 2,4'-MDA. The 3,000 generated conformations are represented in grey, the clustering representative conformation are labeled with letters that correspond to the structures in Figures S-24 and S-25. The asterisk indicates the structures that are shown in the manuscript.

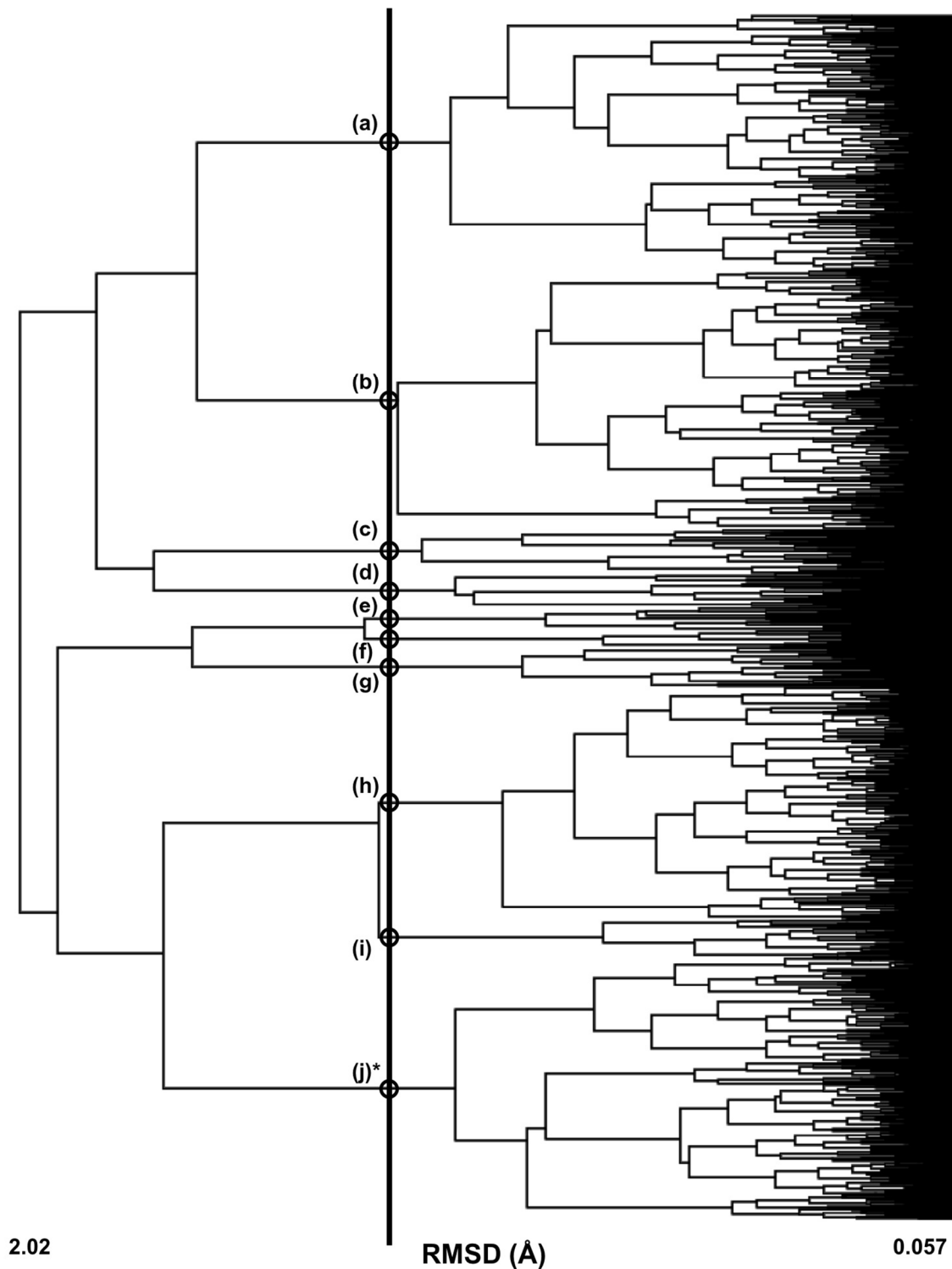


Figure S-24. Clustering analysis of 3,000 conformations of the ring protonated 2,4'-MDA. Clustering is based on root mean square distance of atoms of superimposed structures. The vertical black bar indicates the RMSD cutoff (1.25 Å) used to select the conformations (circled) for further analysis. The asterisk represents the structures shown in the paper.

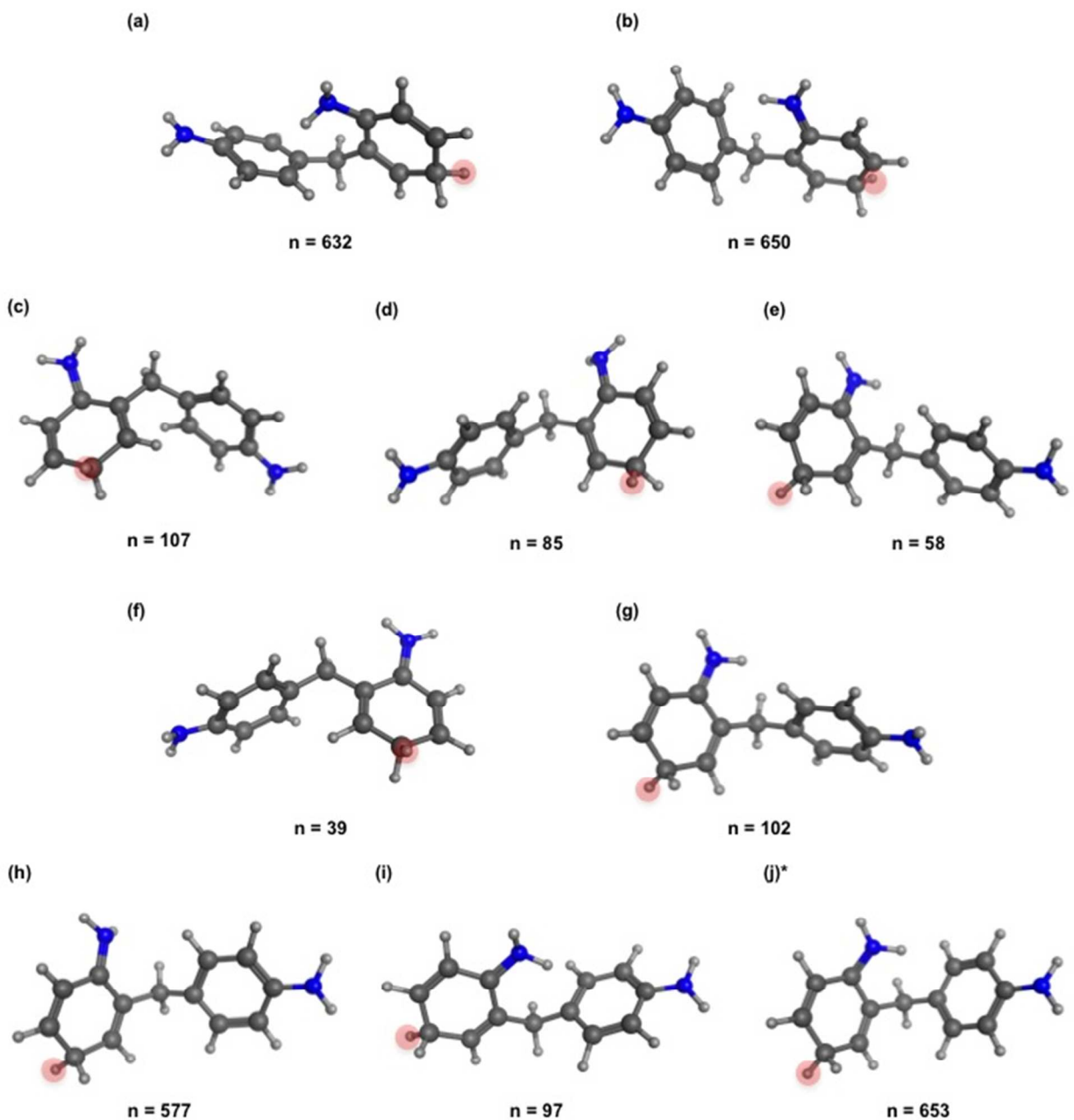


Figure S-25. Representative conformations of the ring protonated 2,4'-MDA generated from an elevated temperate molecular dynamic protocol. Carbon atoms are shown in dark grey, hydrogen in light grey, and nitrogen in blue. The asterisk represents the structures shown in the paper. The number of conformations each of these represents from clustering is shown below the conformation.